MAGNETIC RESONANCE IN CHEMISTRY
Magn. Reson. Chem. **36**, S61–S70 (1998)

^{7}Li solid-state NMR of lithium amides: structural information from ^{7}Li quadrupolar coupling constants†

Michael Hartung,[1] Harald Günther,[1]* Jean-Paul Amoureux[2] and Christian Fernandéz[2]

[1] University of Siegen, FB 8, OC II, D-57068 Siegen, Germany
[2] Université des Science et Techniques de Lille, F-59655 Villeneuve d'Ascq Cedex, France

Received 15 December 1997; revised 6 February 1998; accepted 10 February 1998

ABSTRACT: Lithium-7 quadrupolar coupling constants, $\chi(^{7}\mathrm{Li})$, were measured for a number of microcrystalline lithium amides by solid-state ^{7}Li magic angle spinning (MAS) NMR. A linear correlation between $\chi(^{7}\mathrm{Li})$ and the structural N—Li—N angle known from x-ray diffraction work was found: $\chi(^{7}\mathrm{Li}) = (4.1 \pm 0.5) \sphericalangle \mathrm{N—Li—N} - (110.8 \pm 69.0)$. On this basis, structural information for new systems becomes available. For the polymer material $[H_2\overline{C(CH_2)_3\overline{N}}Li]_n$ a ladder structure is proposed. The π-flip of the five-membered metallacycle formed by the coordination of tetramethylethylenediamine (TMEDA) with lithium in $[(H_2\overline{C(CH_2)_3\overline{N}}Li)_2 \cdot \mathrm{TMEDA}]_2$ was detected by ^{13}C cross-polarization/MAS DNMR spectroscopy. From the analysis of the temperature-dependent lineshape of the methyl signals, a barrier of $\Delta G^{\neq}(293) = 66$ kJ mol^{-1} was derived for this rotational process in the solid, which compares favourably with data derived for related compounds. © 1998 John Wiley & Sons, Ltd.

KEYWORDS: NMR; ^{7}Li NMR; solid-state NMR; quadrupolar coupling; structure; lithium amides

INTRODUCTION

Lithium-6,7 NMR is an indispensible tool for structural investigations of organolithium compounds[1] and lithium amides[2] in solution and a large variety of different 1D and 2D NMR experiments are at our disposal.[3] Both lithium nuclides, ^{6}Li ($I = 1$) and ^{7}Li ($I = 3/2$), possess a quadrupole moment, Q, but that of ^{6}Li is much smaller than that of ^{7}Li (-8.2×10^{-4} *vs.* $-4.0 \times 10^{-2}/10^{-28}$ m^2).[4] As a consequence, for many applications ^{6}Li has the more favourable NMR properties and is the nucleus of choice in all cases where narrow resonance lines are needed to measure small chemical shifts or scalar spin–spin coupling constants. On the other hand, owing to its larger quadrupole moment, ^{7}Li has shorter relaxation times which can be an advantage in a number of cases, e.g. if signal sensitivity is a problem.

In solid-state NMR, the quadrupolar coupling constant, χ, is an additional important parameter related to bonding and structure.[5] It depends on the magnitude of Q according to

$$\chi = eQeq/h \qquad (1)$$

where e is the elementary charge, eq is the electric field gradient at the nucleus and h is Planck's constant. Because of its larger magnitude, $\chi(^{7}\mathrm{Li})$ varies more strongly with structure and is, therefore, more sensitive than $\chi(^{6}\mathrm{Li})$.

The importance of quadrupolar interactions in organolithium systems has long been recognized and several early studies dealt with the relationship between $\chi(^{7}\mathrm{Li})$ and the structure of organolithium compounds in the solid.[6] Not much use was made of that approach in this field in the following years, however, until Jackman *et al.*[7] based structural studies in solution on the ^{7}Li quadrupolar splitting constant, QSC, defined by

$$QSC = (1 + \eta^2/3)^{1/2}\chi \qquad (2)$$

where $\eta = (q_{yy} - q_{xx})/q_{zz}$ is the asymmetry parameter and the q_{ii} are the diagonal elements of the electric field gradient tensor for the ^{7}Li nucleus in its principle axis system. QSC data for individual compounds become available through ^{7}Li spin–lattice relaxation measurements, but because in solution η and χ cannot be obtained separately, QSC data are treated only as empirical parameters related to the electronic environment of the respective ^{7}Li nuclei. From experiments with lithium enolates, Jackman *et al.* found typical ranges for the QSCs of aggregates with different size, 40–80 kHz for tetramers and 120–240 kHz for dimers.[8] Later, characteristic differences for QSC values were also found for di- and tetrasolvated dimers of lithium phenolates (270–280 and *ca.* 160 kHz, respectively), which classifies these parameters as additional tools to study solvation phenomena.[9]

Johnels[10] has drawn attention to the potential which $\chi(^{7}\mathrm{Li})$ can have for structural investigations of organolithium compounds. He showed that a comparison between the quadrupolar splitting constant, QSC, as determined in solution (see above) and in the solid

* H. Günther, University of Siegen, FB 8, OC II, D-57068 Siegen, Germany.
E-mail: guenmr@in400.chemie.uni-siegen.de
Contract/grant sponsor: Deutsche Forschungsgemeinshaft.
Contract/grant sponsor: Fonds der Chemischen Industrie.
Contract/grant sponsor: Volkswagen Stiftung.
† Dedicated to Professor John D. Roberts on the occasion of his 80th birthday.

CCC 0749-1581/98/SI0061–10 $17.50

[Eqn. (2)], can give information about structural similarities for solute and solid organometallic systems. Other solid-state ^{6,7}Li NMR studies of organic and organometallic compounds have only recently been reported.[11–17] We have shown that solid-state ^{13}C NMR provides an interesting approach to the study of dynamic processes in solid organolithium compounds.[14] From the measurement of temperature dependent ^{7}Li magic angle spinning (MAS) spectra it was also apparent that changes in the quadrupolar coupling constant accompany these dynamic processes.

In this paper, we report results obtained for lithium amides, where different types of aggregates exist with cyclic and so-called ladder structures. The aim of the study was to investigate what type of structural information can be extracted from the ^{7}Li quadrupolar coupling constant, $\chi(^{7}\mathrm{Li})$, of these systems and examples were therefore chosen according to the availibilty of x-ray data. Our selection includes a helix-type polymeric system $[((H_3C)_2CH)_2NLi]_n$ (**1**),[18] and cyclic oligomers $[(H_3C)_2\overbrace{C(CH_2)_3C(CH_3)_2}NLi]_4$, $[((H_3C)_3Si)_2NLi]_3$, $[((H_3C)_2CH)_2NLi(THF)]_2$ and $[((H_3C)_3Si)_2NLi(O(C_2H_5)_2)]_2$ (**2–5**).[19–22] In addition, oligomers with ladder structure, $[(H_2\overbrace{C(CH_2)_3}NLi)_2 \cdot TMEDA]_2$ (**6**)[23] and $[H_2\overbrace{C(CH_2)_5}NLi]_6$ (**7**)[24] were investigated. A compound with unknown structure, the presumably polymeric material $[H_2\overbrace{C(CH_2)_3}NLi]_n$ (**8**), obtained by reaction of pyrrolidine with butyllithium in hexane,[23] was also included for testing the possibilities of structure elucidation by NMR (Scheme 1). We also report ^{6}Li, ^{13}C and ^{15}N NMR data for these systems.

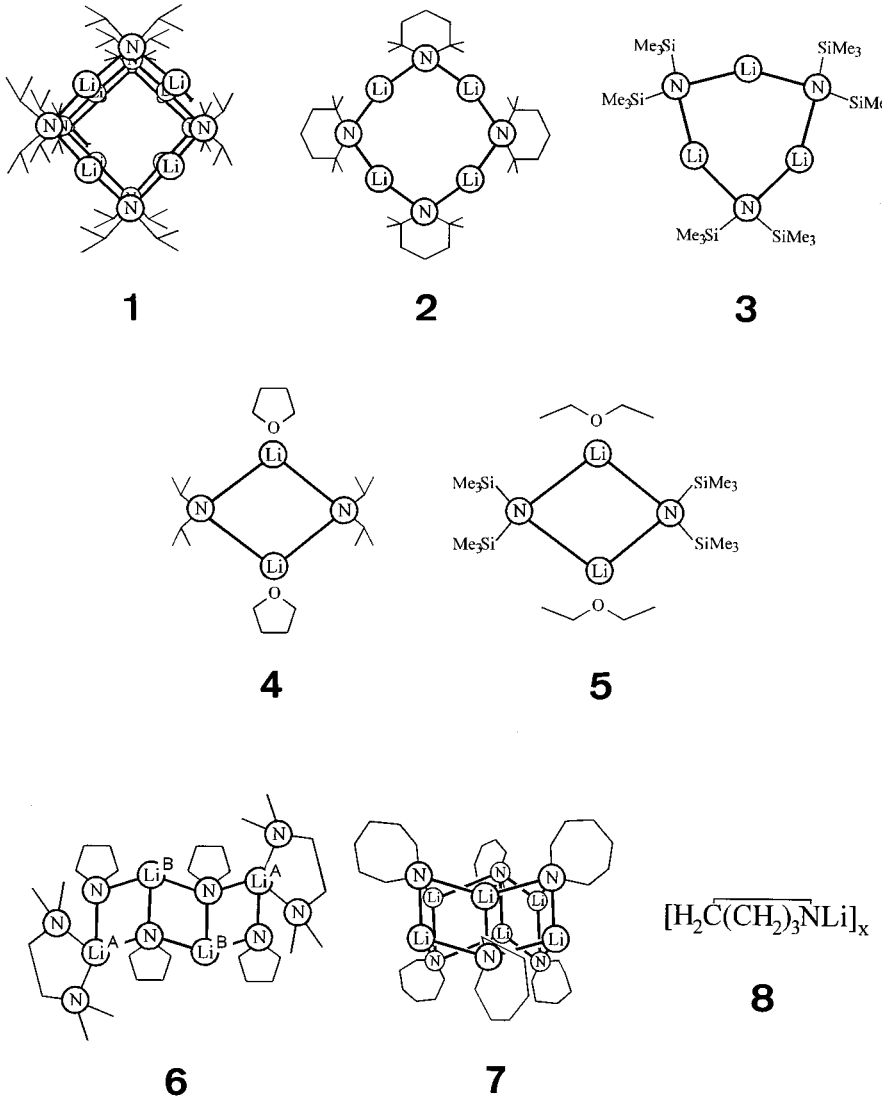

Scheme 1. Lithium amides with cyclic structures.

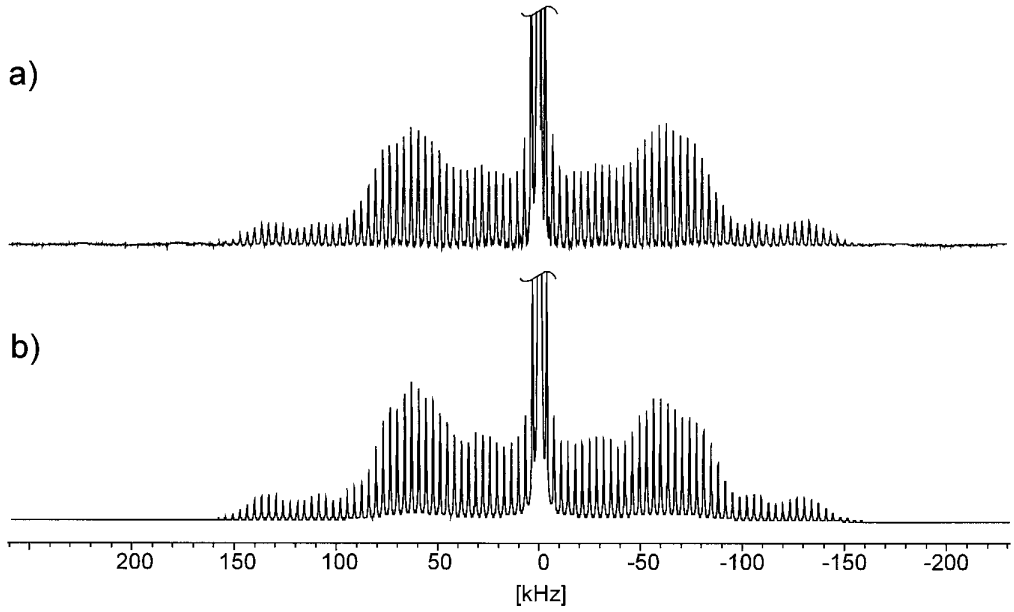

Figure 1. 116.589 MHz ^{7}Li MAS spectrum of $[((H_3C)_3Si)_2NLi \cdot OEt_2]_2$ **(5)**; rotational frequency 3.5 kHz; 5000 transients. (a) Experimental; (b) QUASAR simulation with $\chi = 298$ kHz, $\eta = 0.2$, $\Delta\sigma = -42$ ppm, η(CSA) = 1.0, exponential line broadening 320 Hz.

RESULTS AND DISCUSSION

^{7}Li MAS NMR spectra were measured for powder samples at spinning speeds of 5–12 kHz. Typical sideband patterns (Fig. 1) were observed and analysed by first-order treatment with respect to the quadrupolar coupling constant $\chi(^7\text{Li})$ and the asymmetry parameter $\eta(^7\text{Li})$ according to[25]

$$\chi(^7\text{Li}) = (2/3)I\,\Delta\nu'_{\text{TS}} \quad (3)$$

and

$$\eta(^7\text{Li}) = 1 - (2\,\Delta\nu'_{\text{PS}})/\Delta\nu'_{\text{TS}} \quad (4)$$

where I is the nuclear spin quantum number, $\Delta\nu'_{\text{TS}}$ is the width of the sideband pattern and $\Delta\nu'_{\text{PS}}$ is the frequency difference between the inner singularities of the sideband envelope. Independently, $\chi(^7\text{Li})$ and $\eta(^7\text{Li})$ were determined by simulating the observed spectra with the program QUASAR.[26] For the present case, we optimized only $\chi(^7\text{Li})$, the ^{7}Li chemical shift anisotropy, and the asymmetry parameters in order to limit the number of unknowns in the fitting procedure. In addition, for simplicity we assumed a collinear orientation of the quadrupolar tensor with respect to the CSA tensor. Any influence of dipolar couplings was neglected. The results of both treatments agree closely, as shown in Table 1. In the following discussion, the values obtained from the spectral simulations with QUASAR are used.

Starting with the data for the structures of Scheme 1 in Table 1, the $\chi(^7\text{Li})$ values observed range from 298 to 610 kHz and show significant differences for the structures studied. A dramatic variation with structure is observed for the two aggregates of lithium diisopropylamide, **1** and **4**, where the polymer shows, to the best of our knowledge, the largest $\chi(^7\text{Li})$ value so far observed. A simple qualitative comparison of the spectra of both systems demonstrates the sensitivity of the solid-state ^{7}Li MAS spectrum for structural variations (Fig. 2). From the data in Table 1, one sees that a nearly linear arrangement of the N—Li—N structural fragment in **1** leads to the largest value for $\chi(^7\text{Li})$ (610 kHz). A decrease in the N—Li—N angle due to the cyclic structure of **2** renders $\chi(^7\text{Li})$ smaller (600 kHz). This trend continues with the cyclic trimer **3** (456 kHz) and the dimers **4** and **5** (360 and 298 kHz, respectively).

In view of the known relationship between χ and the bond geometry,[27] as exemplified by the correlation between $\chi(^{17}\text{O})$ and the Si—O—Si bond angle in silicates,[28] it was reasonable to correlate the $\chi(^7\text{Li})$ values of **1–5** with the N—Li—N angles from the x-ray structures. One finds a linear correlation (Fig. 3) which is described by the following equation ($r = 0.98$):

$$\chi(^7\text{Li}) = (4.1 \pm 0.5) \sphericalangle \text{N—Li—N} - (110.8 \pm 69.0) \quad (5)$$

Thus, on this basis the N—Li—N angle of aggregates with unknown structure may be estimated [$< \text{N—Li—N} = 0.24\ \chi(^7\text{Li}) + 27.2$] and information about the aggregation state of lithium amides can be derived. It must be pointed out, however, that an angle dependence of the asymmetry parameter η has been reported for ^{17}O data in silcate glasses[29] and this aspect was neglected for $\eta(^7\text{Li})$ in the present study. From the data in Table 1, one sees that η varies little for the compounds investigated here, with the exception of system **4**. The data for **4** deviate from the linear plot more than those of the other compounds and further investigations with systems of different structure are therefore necessary to clarify this point. If we neglect the results for **4**, the linear correlation is slightly improved with respect to the error in the intercept:

$$\chi(^7\text{Li}) = (4.6 \pm 0.4) \sphericalangle \text{N—Li—N} - (187.7 \pm 63.0) \quad (6)$$

Table 1. ^{7}Li quadrupolar coupling parameters and CSA data ($\Delta\sigma$, η) for twofold coordinated lithium amides

Compound	No.	Structure	<N—Li—N (°)	Ref. for x-ray data	$\chi(^{7}\text{Li})[\text{kHz}]/\eta(^{7}\text{Li})$ Eqns (3) and (4)	$\chi(^{7}\text{Li})[\text{kHz}]/\eta(^{7}\text{Li})$ QUASAR	$\Delta\sigma(^{7}\text{Li})$ (ppm)/ η(CSA)(^{7}Li): QUASAR
Helix polymer:							
$[((H_3C)_2CH)_2NLi]_n$	**1**	Helix	176	18	610/0.1	610/0.1	−40/0.0
Cyclic oligomers:							
$[(H_3C)_2\overline{C(CH_2)_3C(CH_3)_2NLi}]_4$	**2**	Tetramer	169	19	576/0.1	600/0.0	−50/0.0
$[((H_3C)_3Si)_2NLi]_3$	**3**	Trimer	147	20, 21	448/0.1	456/0.1	−46/0.0
$[((H_3C)_2CH)_2NLi \cdot THF]_2$	**4**	Dimer[a]	107	22	368/0.6	360/0.6	−55/1.1
$[((H_3C)_3Si)_2NLi \cdot O(C_2H_5)_2]_2$	**5**	Dimer	105	19	314/0.2	298/0.2	−42/1.0

[a] $T = 213$ K.

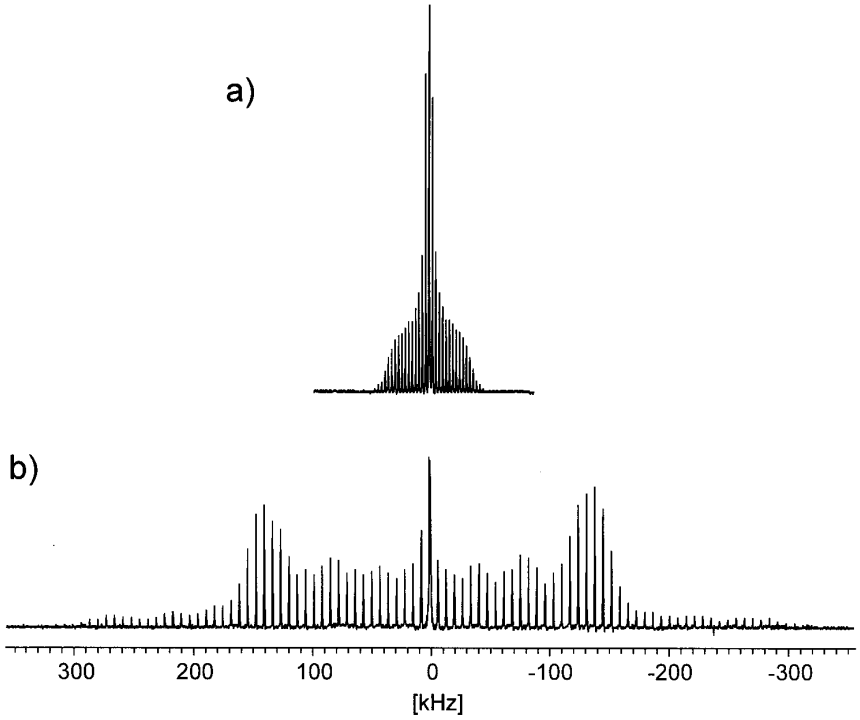

Figure 2. Comparison of the 116.59 MHz MAS room temperature spectra of compounds **4** (a) and **1** (b). Rotational frequencies 2.8 and 7.0 kHz, respectively; number of transients 128.

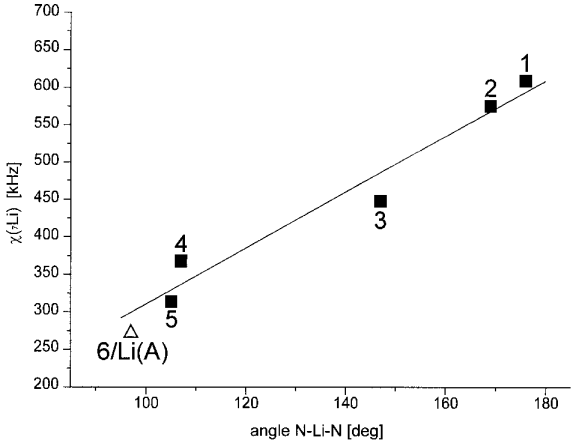

Figure 3. Correlation between the quadrupolar coupling constant $\chi(^7Li)$ of **1–6** and the structural N—Li—N angle derived from X-ray data {cf. Table 1 and text for the result for Li(A) in compound **6** [Δ]}.

Furthermore, the quadrupolar coupling constant may also be influenced by the nature of the donor atoms involved, where we have oxygen for the additional ligands in **4** and **5**.

Turning now to structures **6–8**, the experimental results are given in Table 2. The data for **6** and **7** were not included in the $\chi(^7Li) \not\propto$ N—Li—N correlation because here lithium sites are coordinated to three nitrogens instead of only two in **1–5**. This should affect the electron distribution around the ^{7}Li nucleus and thus the quadrupolar coupling constant. In addition, for **6** we have two different nitrogen sites, Li(A) and Li(B). Both spinning sideband patterns are superimposed (Fig. 4) and only the larger of the two quadrupolar coupling constants (362 kHz, see Table 2) could be derived from the MAS spectrum with the help of Eqns (3) and (4). The small chemical shift difference (0.4 ppm), which was resolved in the solid only for a sample labelled with ^{6}Li [Fig. 5(a)], prevented the application of one of the various 1D and 2D methods proposed to separate overlapping sideband patterns in solid state NMR spectra. Furthermore, these methods, even if they were applicable, would not yield the assignment of the two $\chi(^7Li)$ values to the lithium sites in structure **6**. We therefore reverted to additional measurements in solution in

Table 2. ^{7}Li quadrupolar coupling parameters and CSA data ($\Delta\sigma$, η) for threefold coordinated lithium amides

Compound	No.	Structure	$\chi(^7Li)$[kHz]/$\eta(^7Li)$ Eqns (3) and (4)	$\chi(^7Li)$[kHz]/$\eta(^7Li)$ QUASAR	$\Delta\sigma(^7Li)$ (ppm)/ η(CSA)(^{7}Li): QUASAR
Oligomeric ladder structures:					
$[(H_2\overline{C(CH_2)_3}NLi)_2 \cdot TMEDA]_2$	**6**	Ladder	362	—	—
$[H_2\overline{C(CH_2)_3}NLi]_2$	**7**	Cyclic ladder	310/0.7	295/0.7	−20/2.0
Polymeric ladder structure:					
$[H_2\overline{C(CH_2)_3}NLi]_n$	**8**	Ladder[a]	348/0.8	350/0.7	−20/1.0

[a] Assumed structure.

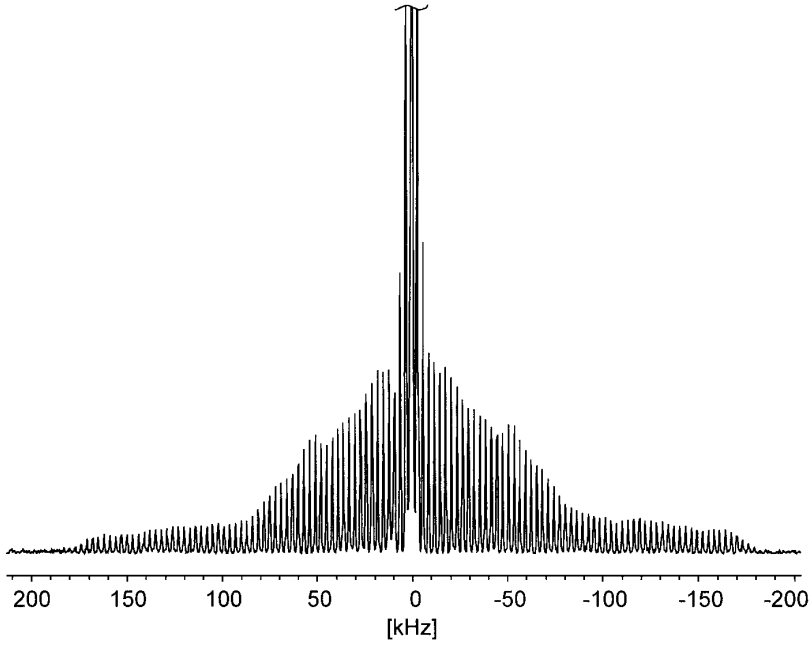

Figure 4. 116.589 MHz ^{7}Li MAS spectra of $[(H_2\overline{C(CH_2)_3NLi})_2 \cdot TMEDA]_2$ (**6**). Rotational frequency 3.5 kHz; sweep width 416 kHz; 242 transients.

order to determine also the smaller $\chi(^{7}Li)$ value for **6** and unequivocally assign the $\chi(^{7}Li)$ data to the two lithium sites (see the next section). Finally, for **8** no x-ray data are available.

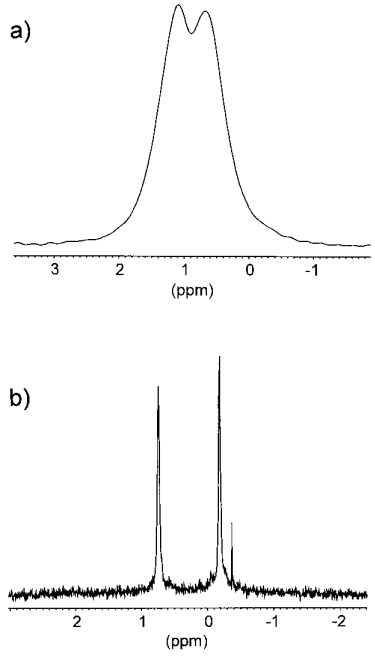

Figure 5. Solid-state MAS and solution-state ^{6}Li spectra of **6** at 44.42 and 58.88 MHz, respectively. (a) Solid-state spectrum with 256 transients, rotational frequency 10 kHz, 293 K, reference solid LiBr; the chemical shift difference between the two lines is 0.4 ppm (17.8 Hz). (b) Saturated solution in toluene-d_8, four transients, 194 K, reference 1 M LiBr in THF; chemical shift difference 0.92 ppm (54.2 Hz).

Combination of solid-state and solution data

In order to analyse the situation for **6**, where two lithium sites exist, we used the following approach. As outlined above, the quadrupolar splitting constant for ^{7}Li, QSC, may be obtained in solution for ^{7}Li by the method introduced by Jackman *et al.*.[7] The original method is restricted to systems where one can determine the molecular correlation time independently from suitable ^{13}C relaxation data. In our case, this problem simplifies because we know already the larger one of the two quadrupolar coupling constants from the solid state measurement (Table 2). Therefore, only the ratio of the two χ values is needed.

From the theory of quadrupolar relaxation, we have[34]

$$1/T_{1q} = (3/2)\pi^2(QSC)^2\tau_c \tag{7}$$

where τ_c is the correlation time for molecular reorientation. Assuming the same τ_c for the two lithium sites A and B in **6**, which is reasonable, we derive

$$\frac{T_{1q}(B)}{T_{1q}(A)} = \frac{QSC(A)}{QSC(B)} \tag{8}$$

If we further assume $\eta(A) = \eta(B)$, which may introduce an error of not more than 15%, and which is justified in the present case according to results from calculations based on a point charge model,[35] Eqn (8) simplifies with Eqn (2) to

$$\chi(A)/\chi(B) = [T_{1q}(B)/T_{1q}(A)]^{-1/2} \tag{9}$$

In solution, the signals of both lithium sites are also separated at low temperature[23] [Fig. 5(b)] and an inversion–recovery experiment modified to take slow chemical exchange into account[36,37] was used for the T_{1q} measurements. In order to insert these data into

Eqn (9), an assignment of both ^{7}Li resonances to the 'inner' and 'outer' Li site of **6** was necessary. For this purpose, the ^{6}Li-labelled compound was synthesized with partial ^{15}N labelling and the signal assignment was based on the ^{15}N satellites observed in the ^{6}Li spectrum. The satellites differ because Li(B) can couple to three nitrogens, whereas Li(A) can couple to only two. This part of the work is described in more detail in the Experimental section. ^{6}Li was chosen because of the smaller linewidth, which allows the ^{15}N satellites to be detected. The results showed that the 'inner' lithium, Li(B), resonates at lower field. We then found $T_{1q}(A) = 0.23 \pm 0.02$ s and $T_{1q}(B) = 0.13 \pm 0.02$ s, which yield, according to Eqn (9), $\chi(A)/\chi(B) = 0.75 \pm 0.16$. With $\chi(B) = 362$ kHz from the solid-state work, $\chi(A) = 272 \pm 35$ kHz results. This value is in good agreement with the prediction based on our empirical Eqn (5) and the N—Li—N angle of 97° determined by x-ray diffraction, which yields 287 kHz (see also Fig. 3).

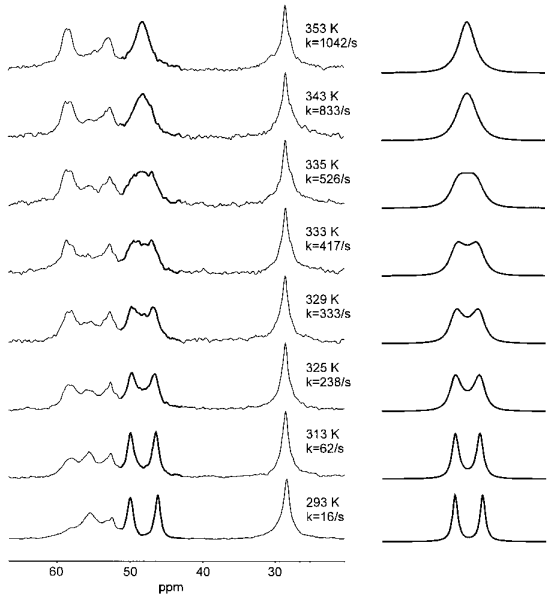

Figure 6. Temperature dependence of the 75.44 MHz CP/MAS ^{13}C spectrum of **6**. Experimental (left) and calculated (right) lineshape for the methyl signals; 512 transients; rotational frequency 3 kHz.

Structure of polymer 8

From the stoichiometric composition, a ladder structure is highly probable for the polymer **8**. Our results for **6**, on the other hand, show that the value of 362 kHz for χ[Li(B)] can be regarded as typical for the tri-coordinated lithium in the lithium amide ladder structures. For **8** we find a χ value of 350 kHz (Table 2), which strongly supports a ladder structure **9**, where lithium is uniformly tri-coordinated, for this material.

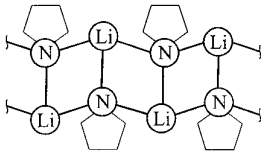

9

Conformational mobility in 6

We have shown that conformational mobility in solid organolithium compounds can be analysed by solid-state NMR and in particular dynamic processes associated with the five-membered metallacycle formed by Li–TMEDA complexation, viz. ring inversion of the half-chair (**a** → **b**) and a 180° rotation or π-flip (**c** → **d**), have been detected:[14]

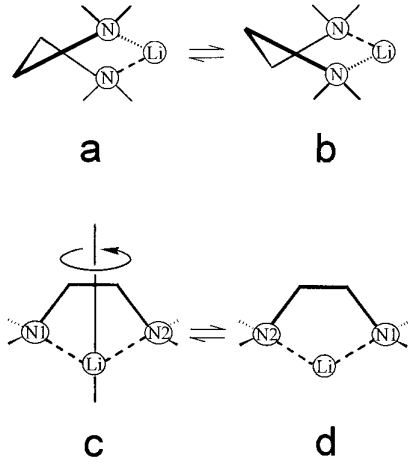

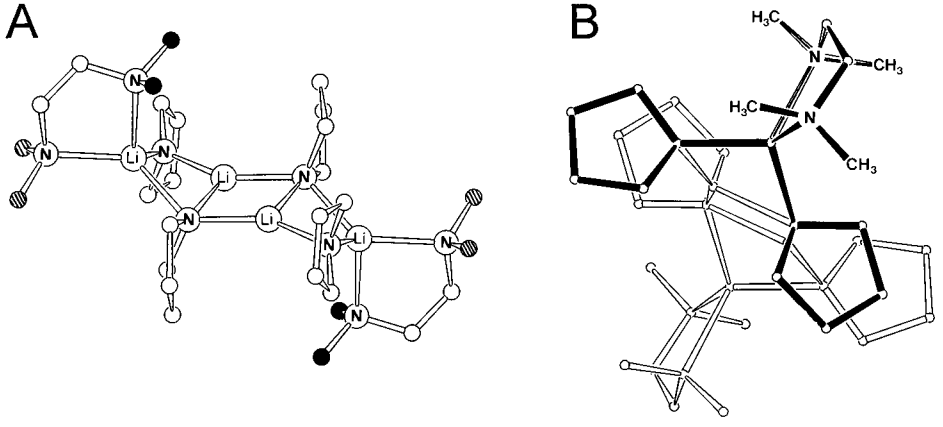

Figure 7. Stereochemistry of **6** according to x-ray results from Ref. 23.

Table 3. ^{13}C chemical shifts δ (ppm)[a] of lithium amides **1–8**

1	2	3	4	5	6	7	8
NCH(CH_3)	NC(CH_3)$_2$	NSi(CH_3)$_3$	NCH(CH_3)	OCH_2CH$_3$	NCH_2CH$_2$	NCH_2CH$_2$	NCH_2CH$_2$
47.8	52.4	8.0	52.8	60.5	52.3	56.8	52.0
NCH(CH_3)	CCH_2CH$_2$		NCH(CH_3)	OCH$_2$CH$_3$	NCH$_2$CH$_2$	NCH$_2$CH$_2$	NCH$_2$CH$_2$
29.7, 24.6	43.9, 40.9		28.0	13.5	28.1	36.2	27.6
	NC(CH_3)$_2$		OCH_2CH$_2$	NSi(CH_3)$_3$	(H_3C)$_2$NCH_2	CH$_2$CH$_2$CH$_2$	
	34.0, 33.3, 32.6		69.2	6.4, 3.9	55.3	27.4	
	CCH_2CH$_2$		OCH$_2$CH$_2$		(H_3C)$_2$NCH$_2$		
	19.8		26.1		49.8, 46.0		

[a] Relative to external TMS.

In this respect, it was of interest that the ^{13}C cross-polarization (CP)/MAS spectrum of **6** showed temperature-dependent lineshape changes which indicated a π-flip for the TMEDA ligands of Li(A). As shown in Fig. 6, the two ^{13}C signals of the TMEDA methyl groups (46.0 and 49.8 ppm relative to TMS) observed at 293 K coalesce at *ca.* 335 K. Consulting the x-ray structure[23] as given in Fig. 7, it is reasonable to assign the two methyl signals to the *endo*- and *exo*-type CH_3 groups marked with full and shaded circles in Fig. 7(A), respectively, which reside in different environments. A π-flip of the TMEDA ligand will exchange these positions. As is apparent from Fig. 7(B), the environment of the two CH_3 groups attached to *one* nitrogen is not exactly identical because of the C_i symmetry of the compound, but very similar, especially if one considers a fast inversion process of the twisted metallacycle. Thus, the chemical shift difference should be smaller than that observed ($\Delta\delta = 3.8$ ppm) and can be associated with the difference between *endo*- and *exo*-type positions. For the lineshape analysis an absolute assignment of the resonances is not necessary and a calculation on the basis of the Gutowsky–Holm equation[38] assuming a two-site exchange system yielded Eyring activation parameters of $\Delta H^{\neq} = 77.2 \pm 6.0$ kJ mol^{-1}, $\Delta S^{\neq} = 38.7 \pm 18.3$ J mol^{-1} K^{-1} and $\Delta G^{\neq}(293) = 65.9 \pm 11.4$ kJ mol^{-1}. The last value compares favourably with the barriers determined earlier[14] for π-flips of the TMEDA ligand in phenyllithium [$\Delta G^{\neq}(326) = 68$ kJ mol^{-1}] and dilithio naphthalene [$\Delta G^{\neq}(317) = 64$ kJ mol^{-1}]. According to these results, the conformational process of the TMEDA π-flip seems not much affected by the different crystal structure.

Table 4. ^{6}Li chemical shifts δ (ppm)[a] of lithium amides **1–8**

Compound	δ (^{6}Li)	Compound	δ (^{6}Li)
1	2.9	**5**	0.7
2	2.0	**6**	0.2 Li(A); 0.6 Li(B)
3	1.1	**7**	0.2
4	1.8	**8**	0.3

[a] Relative to LiBr–H_2O.

Chemical shift data

For completeness, the ^{13}C, ^{6}Li and ^{15}N chemical shift data for **1–8** are collected in Tables 3–5. Lithium-6 NMR was used for the shift measurements in order to avoid correction for quadrupolar effects which are necessary in case of ^{7}Li measurements.[25]

CONCLUSION

We have shown that the ^{7}Li quadrupolar coupling constant for lithium cations coordinated to two amide nitrogens in lithio amides is linearily correlated with the N—Li—N structural angle; $\chi(^{7}\text{Li})$ can thus yield valuable structural information in cases where x-ray results are lacking owing to the unavailability of suitable crystals or the existence of amorphous compounds. A ladder structure has been derived on this basis for the polymer $[H_2\overrightarrow{C(CH_2)_3}\overrightarrow{N}Li]_n$. In suitable cases, $\chi(^{7}\text{Li})$ data may be derived from the measurement of the $T_{1\rho}$ data in solution if an analysis of the solid-state NMR spectrum is hampered by overlap of the sideband mani-

Table 5. ^{15}N chemical shifts δ (ppm)[a] of lithium amides **1–8**

1	2	3	4	5	6	7	8
NCH(CH_3)	NC(CH_3)$_2$	NSi(CH_3)$_3$	NCH(CH_3)	NSi(CH_3)$_3$	NCH$_2$CH$_2$	NCH$_2$CH$_2$	NCH$_2$CH$_2$
−292.8	−277.0	−349.7	−350.7	−362.1	−344.4, −352.8	−343.1	−348.8
					(H_3C)$_2N$CH$_2$		
					−366.5, −367.8		

[a] Relative to CH_3NO_2.

folds for non-isochronous lithium sites. In addition, the π-flip of the TMEDA ligand in solid $[(H_2\dot{C}(CH_2)_3\dot{N}Li)_2 \cdot TMEDA]_2$ has been detected and characterized by dynamic CP/MAS ^{13}C NMR from the lineshape changes of the methyl resonances.

EXPERIMENTAL

Sample preparation

Powder samples of lithium amides **1–8** were synthesized as described.[18–24]

[^{15}N]Pyrrolidine. ^{15}N-Enriched succinimide was prepared from [^{15}N]urea by a literature procedure[39] modified in order to increase the yield with respect to ^{15}N. A thoroughly ground mixture of 0.25 g of urea (4.0 mmol, 100% ^{15}N) and 0.85 g of succinic anhydride (8.5 mmol) was kept at 180 °C for 1 h in a dry, evacuated, 50 ml glass vial. The resulting brown solid contained 0.61 g of succinimide (6.2 mmol, 78%) together with 0.16 g of succinic anhydride. Without futher purification, 3.10 g of crude product were mixed with 6.90 g of commercial succinimide with ^{15}N in natural abundance. Following a procedure described by Moffett,[40] this mixture was slowly added to 7.6 g (20 mmol) of $LiAlH_4$ in dry THF. The isolated product was purified, yielding 0.86 g (12.0 mmol, 12%) of pyrrolidine (^{15}N content 22%).

Spectra

Solid-state NMR spectra were recorded on a Bruker MSL 300 NMR spectrometer (frequencies 116.60 MHz for ^{7}Li, 75.44 MHz for ^{13}C, 44.15 MHz for ^{6}Li and 30.42 MHz for ^{15}N) equipped with a 4 mm double-tuned MAS probe. Typical 90° pulse lengths were 3.5 μs for ^{6}Li and 2.5 μs for ^{7}Li. Dipolar coupling to protons was removed by continuous-wave ^{1}H high-power decoupling during acquisition. ^{13}C and ^{15}N chemical shifts were obtained from CP/MAS spectra using a 6 ms contact pulse. Spectra were referenced externally to saturated [^{6}Li]Br–H_2O (^{6}Li, ^{7}Li), adamantane (^{13}C) and NH_4Cl (^{15}N), respectively. The spinning speed varied between 1 and 12 kHz according to the spectral widths of the quadrupolar patterns. With the exception of **4**, the samples were measured at room temperature in 4 mm ZrO_2 rotors, charged under argon and sealed with KEL-F caps; **4** was measured at 213 K because the x-ray data were collected at 173 K and NMR measurements indicate a phase transition at 280 K.[35] For further experimental details, see the figure captions.

Solution-state NMR spectra were recorded on a Bruker AMX 400 NMR spectrometer, equipped with a 5 mm triple resonance probe and operating at a ^{6}Li frequency of 58.88 MHz. The 90° ^{6}Li pulse length was 9.5 μs; composite pulse ^{1}H decoupling was used. ^{6}Li NMR spectra were referenced externally to 0.1 M ^{6}LiBr in THF. Saturated solutions of **6** were prepared by dissolving, under argon, the appropriate amount of polycrystalline material in dry toluene-d_8. Data acquisition and processing were performed with standard Bruker NMR software.

Assignment of the ^{6}Li resonances of 6. The NMR signal of the α-carbons of partially enriched [^{15}N]pyrrolidine displays a singlet and a doublet with a splitting of 3.1 Hz due to scalar ^{13}C,^{15}N coupling. The isotopic ^{15}N/^{14}N ratio could therefore be determined from the relative intensity of these signals in the $^{13}C\{^{1}H\}$ NMR spectrum and amounted to 1:3.5, which corresponds to 22% enrichment. Structure **6** contains four nitrogens in the ladder and the statistical weight of the different isotopomers with no, one, two, three or four ^{15}N nuclei, which follows from a Bernoulli-type calculation,[41] is 36.1, 41.9, 18.2, 3.5 and 0.3%, respectively. On this basis, one expects a 1:14:49:14:1 quintet for Li(A) and a 1:14:104:252:104:14:1 septet for Li(B). The theoretical lineshapes which result if one assumes a uniform $^{1}J(^{15}N, ^{6}Li)$ value of 3.45 Hz are plotted together with the experimental spectrum in Fig. 8.

Evidently, the assumption of a uniform $^{1}J(^{15}N, ^{6}Li)$ value holds only for the high-field signal at −0.17 ppm. The multiplet at 0.75 ppm seems to be broadened by slightly different scalar interactions [Fig. 8(a)]. We therefore used the high-field signal and compared the experimental lineshape [Fig. 8(c)] with the theoretical quintet [Fig. 8(b)] and the septet [Fig. 8(d)], respectively. As can be seen from the intensity of the inner satellites, the experimental data fit the quintet best. The signal at −0.17 ppm is therefore assigned to Li(A) and that at 0.75 ppm to Li(B).

The DNMR measurements for **6** were performed with the following parameters: natural linewidth 65 Hz,

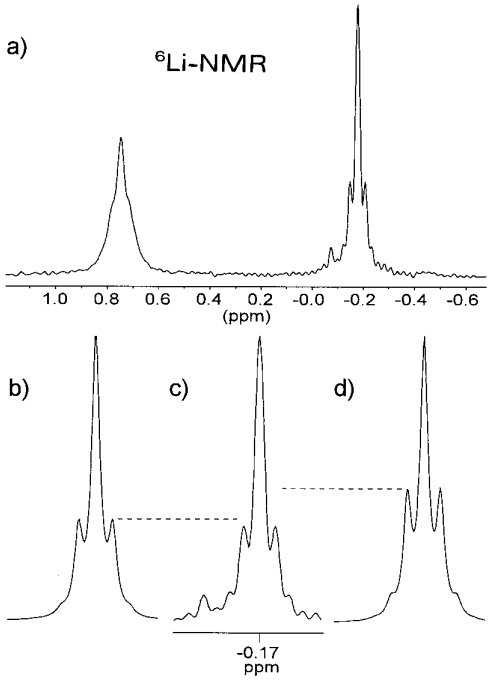

Figure 8. Comparison of the experimental and calculated lineshapes for the ^{6}Li resonances Li(A) and Li(B) in **6**. (a) and (c) experimental in toluene-d_8; one transient, 193 K; (b) calculated quintet; (d) calculated septet (cf. text).

determined in the slow exchange region at 293 K, and chemical shift difference 290 Hz. The temperature calibration was based on phase transitions of standard samples as described.[42]

Acknowledgements

We are indebted to the Deutsche Forschungsgemeinschaft and to the Fonds der Chemischen Industrie for financial support and to the Volkswagen Stiftung for a spectrometer grant.

REFERENCES

1. For a review on solid-state structures, see W. N. Setzer and P. v. R. Schleyer, *Adv. Organomet. Chem.* **24**, 353 (1985).
2. For a review on solid-state structures, see (a) K. Gregory, P. v. R. Schleyer and R. Snaith, *Adv. Inorg. Chem.* **37**, 47 (1991); (b) R. E. Mulvey, *Chem. Soc. Rev.* **20**, 167 (1991).
3. D. B. Collum, *Acc. Chem. Res.* **26**, 227 (1993); H. Günther, in *Encyclopedia of NMR*, edited by D. M. Grant and R. K. Harris, Vol. 5, p. 2087. Wiley, Chichester (1996); H. Günther, in *Advanced Applications of NMR to Organometallic Chemistry*, edited by M. Gielen, R. Willem and B. Wrackmeyer, p. 247. Wiley, Chichester (1996).
4. R. K. Harris, in *Encyclopedia of NMR*, edited by D. M. Grant and R. K. Harris, Vol. 5, p. 3301. Wiley, Chichester (1996).
5. J. A. S. Smith, *Ber. Bunsenges. Phys. Chem.* **91**, 1145 (1987); T. J. Bastow, *Z. Naturforsch., Teil A* **49**, 320 (1993); C. A. Fyfe, *Solid State NMR for Chemists*. CFC Press, Guelph (1983); D. Freude and J. Haase, in *NMR—Basic Principles and Progress*, edited by P. Diehl, E. Fluck, H. Günther, R. Kosfeld and J. Seelig, Vol. 29, p. 1. Springer, Berlin (1994); R. K. Harris, in *NMR and the Periodic Table*, edited by R. K. Harris and B. E. Mann, Chapt. 1. Academic Press, London (1978).
6. E. A. C. Lucken, *J. Organomet. Chem.* **4**, 254 (1965); A. Bernheim, I. L. Adler, B. J. Lavery, D. C. Lini, B. A. Scott and J. A. Dixon, *J. Phys. Chem.* **9**, 3442 (1966).
7. L. M. Jackman, L. M. Scarmoutzos and C. W. Brosse, *J. Am. Chem. Soc.* **109**, 5355 (1987).
8. L. M. Jackman and J. Bortiatynski, in *Advances in Carbanion Chemistry*, edited by V. Snieckus, p. 45. Jai Press, Greenwich, CT (1992).
9. L. M. Jackman and D. Çizmeciyan, *Magn. Reson. Chem.* **34**, 14 (1996).
10. D. Johnels, *J. Organomet. Chem.* **445**, 1 (1993).
11. T. Pietrass, P. K. Burkert and H. M. Karsch, *Z. Naturforsch., Teil A* **47**, 117 (1992).
12. T. Pietrass and P. K. Burkert, *Z. Naturforsch., Teil B* **48**, 1555 (1993).
13. T. Pietrass and P. K. Burkert, *Magn. Reson. Chem.* **31**, 709 (1993).
14. W. Baumann, Y. Oprunenko and H. Günther, *Z. Naturforsch., Teil A* **50**, 429 (1994.
15. D. Johnels, A. Anderson, A. Boman and U. Edlund, *Magn. Reson. Chem.* **34**, 908 (1996).
16. M. Veith, M. Zimmer, K. Fries, J. Böhnlein-Maus and V. Huch, *Angew. Chem.* **108**, 1647 (1996); *Angew. Chem., Int. Ed. Engl.* **35**, 1529 (1996).
17. J. E. Espidel, R. K. Harris and K. Wade, *Magn. Reson. Chem.* **32**, 166 (1994).
18. N. D. R. Barnett and R. E. Mulvey, *J. Am. Chem. Soc.* **113**, 8187 (1991).
19. M. F. Lappert, M. J. Salde and A. Singh, *J. Am. Chem. Soc.* **105**, 302 (1983).
20. D. Mootz, A. Zinnius and B. Böttcher, *Angew Chem.* **81**, 398 (1969); *Angew Chem., Int. Ed. Engl.* **8**, 378 (1969).
21. R. D. Rogers, J. L. Attwood and R. Grüning, *J. Organomet. Chem.* **157**, 229 (1978).
22. P. G. Willard and S. M. Salvino, *J. Org. Chem.* **58**, 1 (1993).
23. D. R. Armstrong, D. Barr, W. Clegg, S. M. Hodgson, R. E. Mulvey, D. Reed, R. Snaith and D. S. Wright, *J. Am. Chem. Soc.* **111**, 4719 (1989).
24. D. Barr, W. Clegg, S. M. Hodgson, G. R. Lamming, R. E. Mulvey, A. J. Scott, R. Snaith and D. S. Wright, *Angew. Chem.* **101**, 1279 (1989); *Angew. Chem., Int. Ed. Engl.* **28**, 1241 (1989).
25. J. P. Amoureux, C. Fernandéz and P. Granger, *NATO ASI Ser., Ser. C* **322**, 409 (1990).
26. J. P. Amoureux and C. Fernandéz, *QUASAR—Solid-State NMR Simulation for Quadrupolar Nuclei*. Lille (1996).
27. C. H. Townes and B. P. Dailey, *J. Chem. Phys.* **17**, 782 (1949); for a review, see Y. A. Buslaev, E. A. Kravcenko and L. Kolditz, *Coord. Chem. Rev.* **82**, 3 (1987).
28. P. J. Grandinetti, J. H. Baltisberger, I. Farnan, J. F. Stebbins, U. Werner and A. Pines, *J. Phys. Chem.* **99**, 12341 (1995).
29. I. Farnan, P. J. Grandinetti, J. H. Baltisberger, J. F. Stebbins, U. Werner, M. A. Eastman and A. Pines, *Nature* **358**, 31 (1992).
30. B. Blümich, P. Blümler and J. Jansen, *Solid State NMR* **1**, 111 (1992).
31. N. Chandrakumar, G. v. Fircks and H. Günther, *Magn. Reson. Chem.* **32**, 433 (1994).
32. S. F. de Lacroix, J. J. Titman, A. Hagemeyer and H. W. Spiess, *J. Magn. Reson.* **97**, 435 (1992).
33. S. C. Shekar and J. A. Hamilton, *Magn. Reson. Chem.* **34**, 433 (1994).
34. J. P. Kintziger and J. M. Lehn, *Mol. Phys.* **22**, 273 (1971).
35. M. Hartung and H. Günther, unpublished results.
36. C. L. Perrin and T. J. Dyer, *Chem. Rev.* **90**, 935 (1990).
37. G. A. Morris and R. A. Freeman, *J. Magn. Reson.* **29**, 433 (1978).
38. H. S. Gutowsky and C. H. Holm, *J. Chem. Phys.* **25**, 1228 (1965).
39. G. C. Crockett, B. S. Swanson, D. R. Anderson and T. H. Koch, *Synth. Commun.* **11**, 447 (1981).
40. R. B. Moffett, *Org. Synth., Coll. Vol.* **4**, 354 (1963).
41. H. G. Zachmann, *Mathematik für Chemiker*, p. 584. VCH, Weinheim (1979).
42. F. C. Riddell, R. A. Spark and G. V. Günther, *Magn. Reson. Chem.* **34**, 824 (1996).

